QUANTIFIED BRAIN ASYMMETRY FOR AGE ESTIMATION OF NORMAL AND AD/MCI SUBJECTS

L.A. Teverovskiy[1], *J.T. Becker*[2], *O.L. Lopez*[2], *Y.Liu*[1,2,3]

[1]Carnegie Mellon University; [2]University of Pittsburgh Medical Center; [3]Penn State University

ABSTRACT

We propose a quantified asymmetry based method for age estimation. Our method uses machine learning to discover automatically the most discriminative asymmetry feature set from different brain regions and image scales. Applying this regression model on a T1 MR brain image set of 246 healthy individuals (121 females; 125 males, 66 ± 7.5 years old), we achieve a mean absolute error of 5.4 years and a mean signed error of -0.2 years for age estimation on unseen MR images using the stringent leave-15%-out cross validation. Our results show significant changes in asymmetry with aging in the following regions: the posterior horns of the lateral ventricles, the amygdala, the ventral putamen with a nearby region of the anterior inferior caudate nucleus, the basal forebrain, hyppocampus and parahyppocampal regions. We confirm the validity of the age estimation model using permutation test on 30 replicas of the original dataset with randomly permuted ages (with p-value < 0.001). Furthermore, we apply this model to a separate set of MR images containing normal, Alzheimer's disease (AD) and mild cognitive impairment (MCI) subjects. Our results reflect the relative severity of brain pathology between the three subject groups: mean signed age estimation error is 0.6 years for normal controls, 2.2 years for MCI patients, and 4.7 years for AD patients.

Index Terms— age estimation, deformable registration, Alzheimer's disease

1. INTRODUCTION

Changes in brain asymmetry due to normal aging or a pathological neurodegenerative processes can provide insights into brain development and help identify an onset of a neurological condition early [1]. Brain asymmetry has been the focus of many recent studies on both cross-sectional and longitudinal datasets [2, 3, 4, 5]. The limitations of these studies are that they require time and labor intensive process of manually delineating brain structures, or they do not focus on such crucial informative features as size and shape asymmetry of the brain structures.

The work is supported, in part, by NIH P50-AG05133, MH064625, MH01077, AG05133, DA015900-01, and PA Health Department grant 4100027294

We propose a machine learning based method that explores the age-related changes in human brain asymmetry. It uses a comprehensive set of 11.5 million deformation and tensor based asymmetry features computed for every voxel at 4 image scales. Our method combines the strengths of the existing approaches and eliminates many of their limitations. First, our analysis takes into account differences not only in size, but also in shape and location of anatomical structures. Second, it can handle hundreds of subjects and millions of features. Third, the learned age estimation model can be easily evaluated on unseen data. Finally, our method does not require human intervention.

2. DATA

Our dataset consists of structural T1 MR images of 246 subjects. These images were acquired on GE 1.5T Signa scanner between 1999 and 2004 at the University of Pittsburgh Alzheimer's Research Center. The spoiled gradient-recalled (SPGR) volumetric T1-weighted pulse sequence was used with the following parameters, optimized for maximal contrast among gray matter, white matter, and CSF: TE = 5ms, TR = 25ms, flip angle = 40, NEX = 1, slice thickness = 1.5 mm/0 mm interslice. The individuals for the study were selected by neuroradiologists at the University of Pittsburgh Medical Center. No participant has a neurologocal disease and all have similar educational level. Mean age of the participants is 66 years (SD=7.5).

3. METHOD

There are four major steps in our method. First, we deformably register a single reference template to each brain image. Second, we compute asymmetry-based features from the obtained deformation fields. Third, we perform feature screening for the most relevant features out of the 11.5 million computed during the second step. Fourth, we use forward selection to find the best subset of features for a linear regression model that estimates age. Each of the four steps is described in detail below.

Image registration: To prepare images for the fully deformable registration, we perform intensity normalization using a histogram equalization approach implemented in the In-

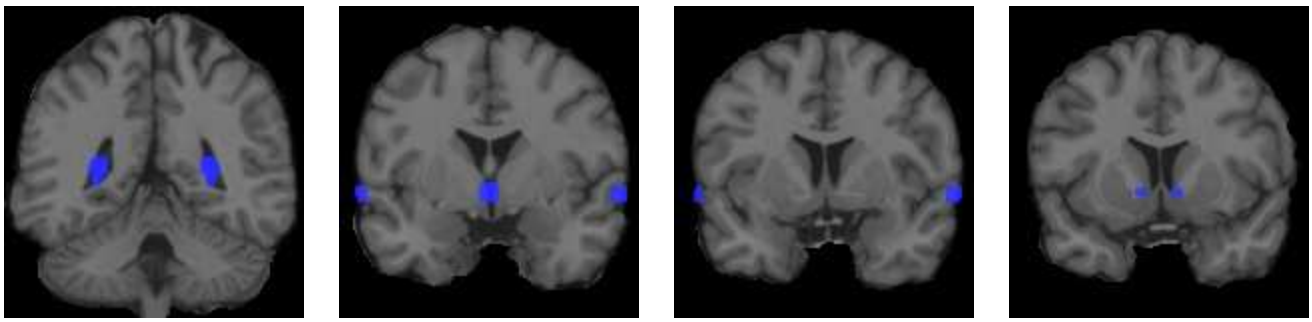

slice 67 slice 111 slice 117 slice 121

Fig. 1. The locations of the top 200 AVR-ranked asymmetry features clustered around posterior horns of the lateral ventricles, the amygdala, the ventral putamen with a nearby region of the anterior inferior caudate nucleus, and the basal forebrain.

sight Toolkit (ITK) [6], followed by midsagittal plane (MSP) alignment [7]. At the last preparatory step, we use MIRIT [8] to affinely register the reference image, *Colin27* template [9], to every image in the dataset. The preliminary steps reduce brightness variations and global differences in overall size, orientation, location and skewing between the images in the dataset. Once the preprocessing is completed, we apply finite element mesh based fully deformable registration algorithm, followed by the asymmetric implementation of Demons fully deformable registration algorithm to register the *Colin27* template to every image [10]. Both of these algorithms are part of ITK. We verify quality of the registration in a quantitatve way using mutual informaton [11].

Asymmetry feature extraction: As the result of the fully deformable registration we obtain deformation fields that contain information about differences in size, shape and locations of the corresponding anatomical structures of the brain images. A deformation field is a vector image that maps reference image voxel coordinates to the coordinates of the corresponding input image voxels. We extract five types of features from these vector fields: x, y, z components, length of the vectors, and the determinant of the Jacobian matrix of the deformation field. This way, for every deformation field we obtain five 3D scalar images, one for each feature type. These images contain information about local differences in x, y, z coordinates and the distances between the corresponding voxels, as well as local contractions/expansions for every voxel neighborhood of the reference image. In order to capture this information with varying degree of locality, we create an image pyramid with 4 image scales for every scalar image obtained. First level in the image pyramid is the image itself, and every subsequent level is a smoothed and subsampled (by the factor of two in each dimension) version of the previous level. At every level of the pyramid we compute an asymmetry image which consists of the absolute value of the voxel-wise difference between voxel values on the left of MSP and their symmetric counterparts on the right. The asymmetry images contain the information of how symmetric each deformation is with regard to five feature types at four image scales. Finally, we compute neighborhood statistics for the voxels in these asymmetry images. We consider a 3x3x3 voxel neighborhood around each voxel and compute mean and standard deviation of the asymmetry image voxel values in this neighborhood. The computed means and standard deviations comprise a pool of available asymmetry-based features. Using mean values in a 3x3x3 voxel neighborhood makes our method less susceptible to registration errors while providing information about local asymmetry, and standard deviation allows us to leverage the information about local inhomogeneities of the deformation fields. The total number of asymmetry features included in our study is 11,479,470.

Feature screening: The image processing and the feature extraction steps transform the database of 246 images into a dataset with 11.5 million asymmetry-based features and 246 data points. Such a large number of features endows our approach with great potential, since it allows us not to restrict the analysis to a particular region of interest, image scale or a feature type. However, this potential can be realized only if we are able to efficiently select a small subset of relevant features from which a generalizable model can be learned. The first step in this process is feature screening, which allows us quickly eliminate vast majority of features non-discriminative features. We rank each feature according to its ability to discriminate between the people in their fifties and people in their seventies, as measured by the augmented variance ratio (AVR) [12]. The larger the AVR, the more discriminative the feature is. Our rationale is that if a feature does not discriminate well between the subjects on opposite ends of the age range, it will not be useful for age estimation. Participants whose ages are between 60 and 69 years old are not used in the feature screening process. Only 200 features with highest AVR make it to the more rigorous forward subset selection.

Forward feature subset selection for linear regression: We use forward selection to learn the linear regression model for age estimation. At each step of forward selection we add the feature that reduces regression error the most. Forward selection insures that even though many of our features are correlated, only the features that contain new information are

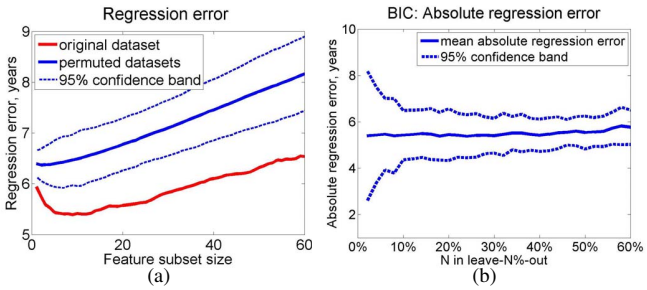

Fig. 2. (a) Age estimation error computed using leave-15%-out cross-validation as a function of feature subset size for original (red) and permuted (blue) datasets selected from 50 asymmetry features with highest AVRs ; (b) absolute age estimation error as a function of the number of subjects left out from THE original dataset for each split. BIC was used for model selection. The age estimation error is robust for up to leave-60%-out cross-validation.

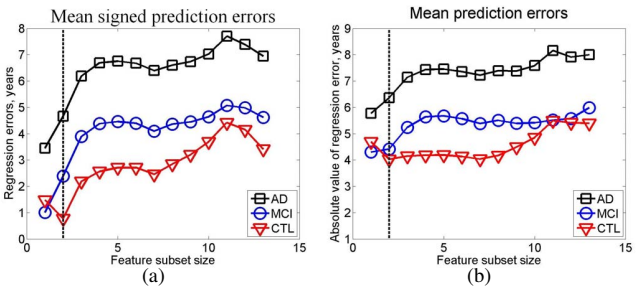

Fig. 3. Mean signed errors (a) and mean absolute errors (b) as a function of feature subset size selected from top 50 AVR-ranked features. The vertical line indicates subset size selected according to the BIC during training on the dataset of 246 normal controls.

added at each step. We use Bayesian Information Criterion (BIC) to determine when the forward selection process should stop. BIC is the goodness of fit for the model penalized by the size of the feature subset the model uses. We use leave-15%-out cross validation with 50 dataset splits to estimate the prediction error of regression models.

4. EXPERIMENTAL RESULTS

The regions where asymmetry is found to change the most with age are the posterior horns of the lateral ventricles, the amygdala, the ventral putamen (and a nearby region of the anterior inferior caudate nucleus), and the basal forebrain (Figure 1). The top features cluster together nicely; no noise filtering was done to produce Figure 1. The cross-validation accuracy, permutation tests and age estimation accuracy on a separate, unseen dataset are described below.

Validation: cross-validation of the linear regression model: The linear regression model chosen using the BIC criterion yields a mean estimation error of 4.1 years on the entire training dataset. Applying cross-validation approach to evaluate predictive capabilities of our method we use 50 $leave-N-out$ splits of the original dataset into training and test sets. The results of the evaluation for different values of N are presented in Figure 2(b). The estimation error remains fairly stable around 5.4 years for N up to 40% (using 148 images for training and 98 images for testing). The standard deviation of the mean estimation errors between the splits first decreases with the increase of the number of images in the test set, and then increases when the number of images in the training set becomes too small to learn a generalizable model.

Validation: permutation test:. In order to show that age estimation accuracy of our model is not achieved due to chance, but rather due to the relationship between aging and brain asymmetry, we perform 30 permutation tests. During each test we randomly permute ages in the dataset, thus destroying any correlation between age and brain asymmetry that is present in the original dataset. For each permuted dataset we learn the regression model and use leave-15%-out cross-validation to estimate prediction errors. The results of leave-15%-out cross validation are presented in Figure 2(a). The mean age estimation error of our model on the 30 permuted datasets was 6.6 years with standard deviation of 0.2 years. These results show that the accuracy of our model on the original dataset is significantly (p-value$<$0.001) higher than that on the permuted datasets.

Validation: age estimation on a new dataset:. We apply the regression model learned on the dataset of 246 normal subjects to a new dataset of 17 AD, 17 MCI and 18 normal controls aged between 50 and 79 years old. The distribution of ages is similar for all three subject classes. The regression model, trained based on the top 50 features, yields larger errors for the AD subjects than for normal controls (Figure 3(b)). Moreover, our results reflect the relative severity of brain pathology between the three subject groups (Figure 3(a)): insignificant age overestimation for normal controls (no pathology, mean signed error is 0.6 years), systematic overestimation of age for MCI patients (mild pathology, mean signed error 2.2 years), and the largest systematic age overestimation for AD patients (severe pathology, mean signed error is 4.7 years). These findings suggest that the brains of AD and MCI patients appear older than that of their normal counterparts. The paired t-test between age estimation errors for the age-matched subjects, revealed that the differences between CTL and AD and CTl and MCI were significant (with p-values of 0.019 and 0.044 respectively), while there was no significant difference between MCI and AD subjects.

5. SUMMARY AND DISCUSSION

Our results show that automatically discovered, quantified asymmetry features sensitive to aging cluster around the posterior horns of the lateral and third ventricles (in agreement

with [13]), the ventral putamen and a nearby region of the anterior inferior caudate nucleus (in agreement with [14, 2, 3], the basal forebrain and superior temporal gyrus(in agreement with [14]) (Figure 1). Basal forebrain is involved in learning and memory function; putamen and inferior caudate nucleus are responsible for executive function. Executive function, memory and ability to learn are known to deteriorate with age. Our findings in ventricular asymmetry changes are most likely indirect evidence of gray matter atrophy in the brain regions that surround the ventricles.

Based on the asymmetry of the selected regions we are able to estimate the age of subjects outside of the training set with an average absolute error of 5.4 years and average signed error of -0.2 years. In addition, when applied to the dataset of AD/MCI/CTL subjects, our model's age estimation errors are consistent with the severity of brain pathology for each subject group. The mean signed error is 0.6 years for normal controls, 2.2 years for MCI patients and 4.7 years for AD patients. These results suggest that AD and MCI patient's brains deteriorate with a higher rate than that of normal controls. In particular, our study indicates that changes in striatum regions and the third ventricle are accelerated for the Alzheimer's disease patients. These findings are consistent with the reports that enlarged third ventricle [15] and amyloid and neurofibrillary changes in the striatum [16] are associated with Alzheimer's disease. We are hopeful that the quantified relationship between brain asymmetry and aging will play an important role in early Alzheimer's disease diagnosis.

While current results are very encouraging, there is room for improvement. In the future, we plan to incorporate more types of features, take into account the signed voxel-wise differences in addition to their absolute values for asymmetry-based features, eliminate the effects of the asymmetry in the reference image, and apply other types of parametric and non-parametric regression for age estimation.

6. REFERENCES

[1] Arthur W. Toga and Paul M. Thompson, "Mapping brain asymmetry," *Nature Reviews Neuroscience*, vol. 4, pp. 37–48, 2003.

[2] Naftali Raz, Ulman Lindenberger, Karen M. Rodrigue, Kristen M. Kennedy, Denise Head, Adrienne Williamson, Cheryl Dahle, Denis Gerstorf, and James D. Acker, "Regional brain changes in aging healthy adults: General trends, individual differences and modifiers," *Cerebral Cortex*, vol. 15, pp. 1676–1689, 2005.

[3] Catriona D. Good, Ingrid S. Johnsrude, John Ashburner, Richard N. A. Henson, Karl J. Friston, and Richard S. J. Frackowiak, "Cerebral asymmetry and the effects of sex and handedness on brain structure: A voxel-based morphometric analysis of 465 normal adult human brains," *Neuroimage*, vol. 14, pp. 685–704, 2001.

[4] Vassili A. Kovalev, Frithjof Kruggel, and D. Yves von Cramon, "Gender and age effects in structural brain asymmetry as measured by mri texture analysis," *Neuroimage*, vol. 19, pp. 895–905, 2003.

[5] Elizabeth R. Sowell, Paul M. Thompson, David Rex, David Kornsand, Kevin D. Tessner, Terry L. Jernigan1, and Arthur W. Toga, "Mapping sulcal pattern asymmetry and local cortical surface gray matter distribution in vivo: Maturation in perisylvian cortices," *Cerebral Cortex*, vol. 12, pp. 17–26, 2002.

[6] L. Ibanez, W. Schroeder, L. Ng, and J. Cates, *ITK Software Guide*, Kitware, Inc., 2005.

[7] Leonid A. Teverovskiy and Yanxi Liu, "Truly 3d midsagittal plane extraction for robust neuroimage registration," in *proceedings of ISBI 2006*, 2006, pp. 860 – 863.

[8] F. Maes, A. Collignon, D. Vandermeulun, G. Marchal, , and P. Suetens, "Multimodality image registration by maximization of mutual information," *IEEE Transactions on Medical Imaging*, vol. 16, no. 2, pp. 187–198, 1997.

[9] J. Mazziotta, A. Toga, A. Evans, P. Fox, J. Lancaster, K. Zilles, R. Woods, and et al, "A probabilistic atlas and reference system for the human brain: International consortium for brain mapping (icbm)," *Philosophical Transactions of Royal Society of London, Section B, Biological Sciences*, vol. 356, no. 1412, pp. 1293–1322, August 2001.

[10] J. C. Gee and D. R. Haynor, *Brain Warping*, chapter Numerical Methods for High Dimensional Warps, Academic Press, 1998.

[11] Leonid A. Teverovskiy, Owen T. Carmichael, Howard J. Aizenstein, and Nicole Lazar amd Yanxi Liu, "Feature-based vs. intensity-based brain image registration: comprehensive comparison using mutual information," in *proceedings of ISBI 2007*, 2007, pp. 576 – 579.

[12] Yanxi Liu, Leonid Teverovskiy, Owen Carmichael, R. Kikinis, M. Shenton, C.S. Carter, V.A. Stenger, S. Davis, Howard Aizenstein, Jim Becker, Oscar Lopez, and Carolyn Meltzer, "Discriminative mr image feature analysis for automatic schizophrenia and alzheimer's disease classification," in *Proceedings of MICCAI 2004*, October 2004, pp. 393 – 401.

[13] M. Matsumae, R. Kikinis, I. Myrocz, A. Lorenzo, T. Sandor, M. Albert, P. Black, and F. Jolesz, "Age-related changes in intracranial compartment volumes in normal adults assessed by magnetic resonance imaging," *Journal of Neurosurgery*, vol. 84, pp. 982–991, 1996.

[14] Danielle J. Tisserand, Martin P.J. van Boxtel, Jens C. Pruessner, Paul Hofman, Alan C. Evans, and Jelle Jolles, "A voxel-based morphometric study to determine individual differences in gray matter density associated with age and cognitive change over time," *Cerebral Cortex*, vol. 14, pp. 966–973, 2004.

[15] I. Slansky, K. Herholz, U. Pietrzyk, J. Kessler, M. Grond, R. Mielke, and W.D. Heiss, "Cognitive impairment in alzheimer's disease correlates with ventricular width and atrophy-corrected cortical glucose metabolism.," *Neuroradiology*, vol. 37, no. 4, pp. 270 – 277, May 1995.

[16] H. Braak and E. Braak, "Alzheimer's disease: striatal amyloid deposits and neurofibrillary changes.," *J Neuropathol Exp Neurol*, vol. 49, no. 3, pp. 215 – 224, May 1990.